Source details

IAENG International Journal of Applied Mathematics

Scopus coverage years: from 2009 to Present
Publisher: International Association of Engineers
ISSN: 1992-9978 E-ISSN: 1992-9986
Subject area: Mathematics: Applied Mathematics
Source type: Journal

CiteScore 2022
1.8

SJR 2022
0.232

SNIP 2022
0.652

View all documents > | Set document alert | Save to source list | Source Homepage

CiteScore | CiteScore rank & trend | Scopus content coverage

¡ Improved CiteScore methodology

CiteScore 2022 counts the citations received in 2019-2022 to articles, reviews, conference papers, book chapters and data papers published in 2019-2022, and divides this by the number of publications published in 2019-2022. Learn more >

CiteScore 2022

$$1.8 = \frac{804 \text{ Citations } 2019 - 2022}{445 \text{ Documents } 2019 - 2022}$$

Calculated on 05 May, 2023

CiteScoreTracker 2023

$$1.6 = \frac{712 \text{ Citations to date}}{451 \text{ Documents to date}}$$

Last updated on 05 August, 2023 • Updated monthly

CiteScore rank 2022

Category	Rank	Percentile
Mathematics — Applied Mathematics	#353/609	42nd

View CiteScore methodology > | CiteScore FAQ > | Add CiteScore to your site

About Scopus

What is Scopus

Content coverage

Scopus blog

Scopus API

Privacy matters

Language

日本語版を表示する

查看简体中文版本

查看繁體中文版本

Просмотр версии на русском языке

Customer Service

Help

Tutorials

Contact us

IAENG International Journal of Applied Mathematics

COUNTRY	SUBJECT AREA AND CATEGORY	PUBLISHER	H-INDEX
Hong Kong Universities and research institutions in Hong Kong Media Ranking in Hong Kong	Mathematics Applied Mathematics	International Association of Engineers	20

PUBLICATION TYPE	ISSN	COVERAGE
Journals	19929978, 19929986	2009-2022

SCOPE

Information not localized

Join the conversation about this journal

Quartiles

FIND SIMILAR JOURNALS

1	2	3	4	5
Engineering Letters	Applied Mathematics and Computation	Journal of Applied Mathematics and Computing	Computational and Applied Mathematics	Interna Differe
HKG	USA	DEU	USA	EGY
54% similarity	39% similarity	36% similarity	36% similarity	

SJR Total Documents Citations per document

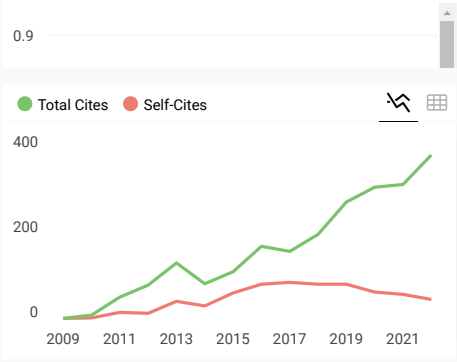

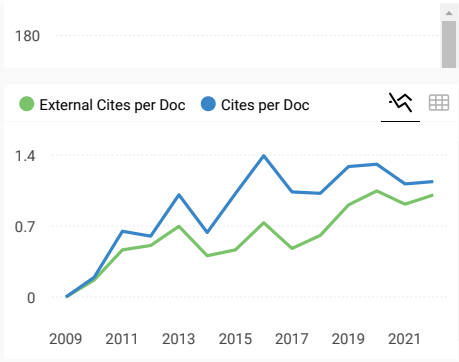

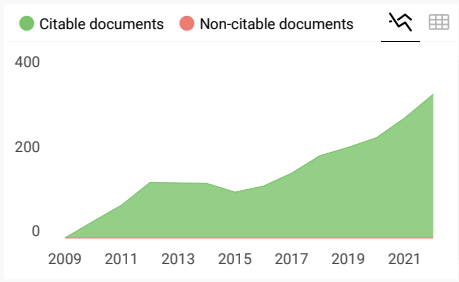

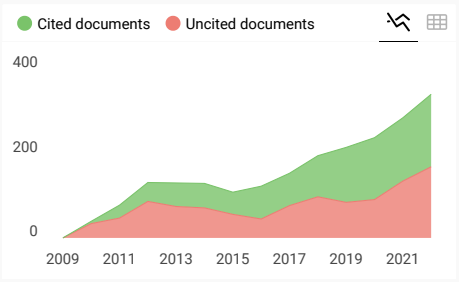

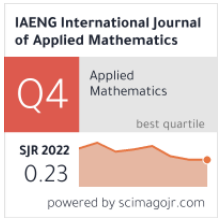

← Show this widget in your own website

Just copy the code below and paste within your html code:

<a href="https://www.scimag

SCImago Graphica

Explore, visually communicate and make sense of data with our **new data visualization tool**.

Metrics based on Scopus® data as of April 2023

L **Long Em Van PHAN** 2 years ago

How to contact to this journal ?IAENG International Journal of Applied Mathematics

reply

SCImago Team

Melanie Ortiz 2 years ago

Dear Long,
Thank you for contacting us.
Unfortunately, we cannot help you with your request.
Best Regards, SCImago Team

M **mahlia** 3 years ago

I have just submitted an article to this journal. I wait the acknowledgment of receipt or directly the decision on the acceptance of the article.

this journal is fee free.

reply

R **Regi** 3 years ago

Publication fee for this journal

Optimizing Hammerstein-Wiener Model for Forecasting Confirmed Cases of Covid-19

Sunusi Bala Abdullahi, *Member, IAENG,* Abdulkarim Hassan Ibrahim, Auwal Bala Abubakar and Abhiwat Kambheera*

***Abstract*—Noise poses challenge to nonlinear Hammerstein-Wiener (HW) subsystem model application, because HW subsystem need large number of parameter interactions. However, flexibility, soft computing, and automatic adjustment to dynamic observation for best model fitting make it potential for forecasting nonlinear data. In this article, we adopted improved HW inference from Levenberg-Marquardt optimization algorithm to optimize HW subsystem and to select best model parameters. Therefore, the adopted model is tested on COVID-19 confirmed reported cases, to estimate transmission rate of COVID-19 virus for period from 15th March 2020 to 29th April 2020. Model validation is carried out on small dataset, which outperforms some existing models. The adopted model is further evaluated using statistical metrics and reported best accuracy of 0.127 and 0.998 for Mean Absolute percentage error (MAPE) and coefficient of determination (R^2) respectively, with best model complexity of 1.86. The obtained results are promising enough in predicting spread of COVID-19 virus and may inspire as guidance to relax lockdown restriction policies.**

***Index Terms*—ANFIS, COVID-19, Hammerstein-Wiener Model, R_o, Least Square method, Levenberg-Marquardt algorithm, Nonlinear System, Machine Learning.**

I. Introduction

THE health authorities in Wuhan reported on 29th December an unusual case of pneumonia [43]. World Health organization (WHO) on 12th March, 2020 declared pneumonia disease as epidemic [1]. Subsequently, virus was designated as 2019 Novel Coronavirus (2019-nCoV-2) from WHO on January 12 and later COVID-19 on 11 February 2020 [2]. Advent of virus-uprising lead to World economic meltdown. According to available data of epidemic disease, number of reported deaths exceeded SARS and Middle East Respiratory Syndrome (MARS) viruses [3]. Clusters of infected people confirmed possibility of human-to-human morbidity [4]. However, transmissions happen between close contacts through respiratory droplets occurred when infected person coughs or sneezes [5]. On 23rd January, virus forced Chinese officials imposed total lockdown in main city of Wuhan before extending lockdown order to neighboring cities. Stay at home order, and travel restrictions are imposed inside and outside china [5], [6]. Virus pandemic lead suspension of world major gatherings. It forced Kingdom of Saudi Arabia to suspends annual holy performances that draws Muslims' pilgrims worldwide. However, Southeast Asia Olympics were also cancelled [3]. As disease continues to spread across the globe, Europe became an epicenter of virus as of March 23, regardless of authorities' actions (includes travel ban, social distancing and stay at home order) [5], [43]. As of 19th February, 2020, 600 people of Diamond princess ship were infected with a short Serial interval of 2.1 days [7] and asymptomatic proportion were estimated as 17.9% [8].

The coronavirus disease was reported by WHO in Africa on 14th of February 2020 in Egypt. It was however, disseminated in west Africa in Ghana on 15th march, 2020. As of 29th April,2020 there were 9413 reported cases of COVID-19 within the west African region [1]. Africa in general has been characterized with poor health care system, lack of infrastructure and low literacy level to tackle the epidemics. There have been numerous call to the stakeholders for improved health care system [9]. Many had forecasted that pandemic would be catastrophic in African region. However, contagious behavior of COVID-19 virus which leads to high rate of disconsolation and deaths, there is a pressing need to analyze COVID-19 virus spreading pattern across the region. Precise forecasting of COVID-19 virus hasten effective technique of applying proactive steps [43]. The proactive steps are regarded as ways to control mortality rate and decrease virus transmission. Authorities have established exit-strategy policies to slack movement restriction order [10]. Precise forecasting of COVID-19 virus may assist governments to prevent further subsequent danger of COVID-19 waves.

Recently, numerous approaches have been proposed and widely used for forcasting and predicting COVID-19 danger, such as basic reproduction number R_0 [6]. Expected cluster of cases caused by primary case over period of time in a susceptible population and exponential growth rate, usually in the initial phase of epidemic grows to exponential pattern is analyzed [11]. In [12] exponential growth rate and maximum likelihood method of estimation is used to estimate R_0 in two different phases 15 Jan. 2020 and 10 Jan. 2020 as 2.56 with 95% C.I.(2.49-2.63) and [13]. 2.24 with 95% C.I.(1.95-2.55) respectively. [14] also use the same method to estimate R_0 as 2.9 with 95% C.I.(2.32-3.63). Likewise [15] use epidemic growth model to estimate R_0 2.1 with 95% C.I.(2-2.2). [16] estimated R_0 using SEIR model as 2.68 with 95% C.I.(2.47-2.86). [17] adopted exponential growth method

Manuscript received November 25, 2020; revised September 12, 2021.

Sunusi Bala Abdullahi is a lead officer at General Investigation, Zonal Criminal Investigation Section, Force Criminal Investigation and Intelligence Department, Nigeria Police, Abuja 900211, Nigeria (e-mail: sbabdullahi@ieee.org)

Abdulkarim Ibrahim Hassan is a PhD Candidate at the Department of Applied Mathematics, King Mongkut's University of Technology, Thonburi, Bangkok, Thailand (e-mail:ibrahimkarym@gmail.com)

Auwal Bala Abubakar is a lecturer at Department of Mathematical Sciences, Faculty of Physical Sciences, Bayero University Kano, Kano 700241, Nigeria and a research associate at the Department of Mathematics and Applied Mathematics, Sefako Makgatho Health Sciences University, Ga-Rankuwa, Pretoria, Medunsa-0204, South Africa (e-mail: ababubakar.mth@buk.edu.ng)

Abhiwat Kambheera is lecturer at Mathematics and Computing Science Program, Faculty of Science and Technology, Phetchabun Rajabhat University, Phetchabun 67000, Thailand (e-mail: apiwat.khu@pcru.ac.th)

Corresponding author: Abhiwat Kambheera, e-mail: apiwat.khu@pcru.ac.th

of estimation, R_0 is 5.7 with 95% C.I.(3.4-9.2). Within the initial outbreak of the disease, R_0 range between 2.0-5.7. Stochastic Susceptible-Infected-Quarantined-Recovered (SIQR) epidemiological model with vaccination effect is evaluated in [22]. However, Susceptible-Infected-Recovered-Dead (SIRD) model used at two different occasions to estimate R_0 with an average of 2.4 is investigated in [18]. Kang et al. employed the same approaches using Susceptible, Infectious and vaccinated to compart a dynamical model of sheep-dog-human brucellosis transmission [27]. In Suebyat et al. [26] developed a mathematical model using fourth-order Runge-Kutta to approximate model solution to risk of airbone infectious diseases such as COVID-19 in outpatient room [26]. The major challenges in assessing variations in basic reproduction number (R_0) among others, includes error due to small number of reported cases, and R_0 fail to consider temporal variations in S.I. during evaluation [10]. Yanuan et al. [20] investigated identify best model of length-of-stay (LoS) hospitalized for patients with COVID-19 in West Sumatra, Indonesia [20].

Moreover, analytical epidemiology models and machine learning techniques such as ANFIS [21] are prone to under fitting or over fitting [19], [23]. Some authors extended usage of Adaptive Neuro-fuzzy Inference System (ANFIS) algorithm [28], [43] to forecast COVID-19 cases, but over parameterization issues of ANFIS, makes parameter estimation very critical. Al'qaness et al. [28] optimize conventional ANFIS according to flower pollination algorithm with Salp Swarm algorithm. This method demonstrates good performance and needs to update layers 4 and 5 according to optimization criteria. Author in [24] proposes an LSTM framework which observes nonlinearity and complexity of COVID-19 time-series data. In ElDahshan et al., [25] extended application of Big data to predict COVID-19 cases, which designs Onto-NoSQL, a Protégé plug-in which handles establishment of Ontology and transformation of a column-oriented NoSQL datastore, this plug-in is implemented to predict COVID-19 prevalence and weather parameters, and the correlation among variability [25]. Large amount of data remains a limitation to this approach. It is very difficult to train accurate machine learning and deep learning models with small datasets. Large dataset is not available for COVID-19 confirmed reported cases in most countries and regions [29]. Henceforth, model that is suitable to a particular geographic data set might not be appropriate to different geographic data set.

Furthermore, as depicted in Figure 2, COVID-19 reported and confirmed cases data are nonlinear in nature, thus complex data structure still needs reliable and computationally efficient (soft computing) forecasting algorithm. However, special interest on identification models in machine learning is rising due to their soft computing and good representation to nonlinear systems. In [30], [31] demonstrated suitability and robustness of Hammerstein and Wiener models in identification of unknown nonlinear dynamic systems. Abdullahi & Gaya [32] demonstrates superiority of H-W models to estimate mobile communication parameters. Likewise, Gonzalez et al. [33] models oxygen dynamics using H-W model. Elnaz et al., [34] extended H-W model estimator to develop and control magnetorheological fluid haptic device. Also, work of Zambrano et al. [35] identified W-H models in a single

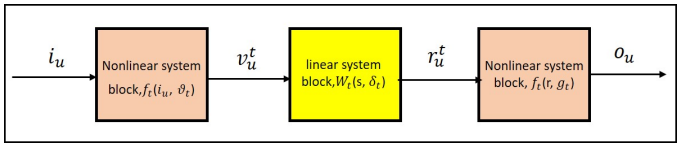

Fig. 1: A general principle of Hammerstein-Wiener model

step. Inspires by literature in [19], [28], [29] and the pressing needs to have a reliable automatic COVID-19 confirmed cases estimation algorithm. Our paper aims to estimate transmission rate of COVID-19 virus according to confirmed reported cases by applying nonlinear Hammerstein-Weiner Model (NL-LTI-NL) with Levenberg-Marquardt (HW-LM) optimization. HW-LM model is easy to implement compared to neural networks such as LSTM, ANFIS and Volterra models. Our adopted model could serve as pilot experiment in relaxing and slacken lockdown strategies. The major Contributions of our paper is itemized as:

1. This paper established a robust identification and forecasting model for confirmed cases of COVID-19 in West African region. 2. Optimized H-W model is adopted according to iterative gradient search method, using Levenberg-Marquardt algorithm. 3. Our extended model is compared with conventional H-W, and ANFIS models, respectively.

A. Model Structure

In this section, we describe subsystem of Hammerstein-Wiener model (H-W). For example, if output observations of model are not linearly dependent on input observations, thus input-output observation relationship can be broken down into many desired subsystems. This system behavior is explained using linear transfer function, and nonlinearities of this system are tracked in accordance with nonlinear functions of inputs and outputs of linear system [36]. H-W has suitable choice for this system function. H-W model as one kind of nonlinear algorithm which combined advantages of Hammerstein and Wiener Model to form one linguistic system, to address individual model's limitations. The two models were linguistically combined in Eqs. (8) and (9), to form a single H-W model. The aim of combining H-W model is to predict transfer function Eq. (2) according to its variables, input nonlinearity, output nonlinearity and its inverse according to actual measurements of , i_u and , o_u, with known internal variables. According to Figure 1, i_u and v_u^t denotes input and output of nonlinear system, where w_t as an internal variable to define input and output of the linear block, with $f_t(i_u, \vartheta_t)$ nonlinear function which transforms , i_u to v_u^t, and $w_t(s, \delta_t)$ denotes linear transfer function parameterized for a given numerator and denominator orders n_{x_t} , n_{y_t}, which transforms v_u^t to r_u^t, then $f_t(r_u, g_t)$ models r_u^t to the system output , o_u. But ϑ_t is denoted by λ_t. The Hammerstein (H) and Wiener (W) models are parameterized using vectors $\boldsymbol{\delta_t} \in R_{x_t}^n$, $\boldsymbol{\delta_t} \in R_{y_t}^n$, W_t, and $\boldsymbol{\theta}$ denotes linear time invariant and vector that accommodate parameterization, which consists of sub-vectors $\boldsymbol{\theta_1}, \ldots, \boldsymbol{\theta_n}$ to parameterize model blocks. s^{-1} denotes inverse shift operator is defined as,

$$s^{-1} v_t = v_{t-1} \tag{1}$$

Therefore, a brief review of the procedures adopted in [37] is presented to develop H-W model. The nonlinear and Linear

Time Invariant (LTI) subsystem can be formulated in time domain with *ni* and *no* number of inputs and outputs of the system, therefore discretized time domain transfer function matrix can be shown:

$$W_t(s,\delta_t) = \frac{Y_t(s,\delta_t)}{X_t(s,\delta_t)} = \frac{y_0^t s^{-1} + y_1^t s^{-1} + \cdots + y_{n_{y_t}}^t s^{-n_{y_t}}}{1 + x_1^t s^{-1} + x_1^t s^{-1} + \cdots + x_{n_{x_t}}^t s^{-n_{x_t}}} \quad (2)$$

$$\delta_t = [y_0^t \cdots y_{n_{y_t}}^t, x_1^t \cdots x_{n_{x_t}}^t] \quad (3)$$

Where $t = 1, 2, \cdots, n_0$ and $c = 1, 2, \cdots, n_i$. And n_x , n_y and n_w denotes zeros, poles of LTI block and delay between *i(t)* and *o(t)* according to number of samples. Therefore, for *t-th*, H-model component is defined as an operator $Q_u\boldsymbol{\theta_u}$ on i_u based on its scalar i_u sequence and similar o_u sequence.

$$o_u = Q_u\boldsymbol{\theta_u} i_u \quad (4)$$

Equation (3) is parameterized using real valued components according to vector, as follows:

$$\boldsymbol{\theta_u} = [\delta_t, \lambda_t] \quad (5)$$

Which is expressed in terms of (3) with

$$o_u = W_t(s, \boldsymbol{\delta_t}) i_u^t \quad (6)$$

where

$$x_u^t = f_t(i_u, \lambda_t) \quad (7)$$

accordingly, function $f_t(..\lambda_t)$ indicates memoryless nonlinear mapping, where restriction is only set at derivatives, $\forall$ elements in λ_u^c included in vector λ_t parameterizes f_t, $\frac{\partial}{\partial \lambda_u^t} f_t(i_u, \lambda_t)$.

According to equations (4) and (6), the general output of nonlinear model can be mathematically formulated in Eq. (8), when zero mean ς_u is independently and identically distributed normally, stochastic approach denoting measurement disturbances formed according to rational noise model.

$$o_u = (\prod_{t=1}^{n} Q_t\boldsymbol{\theta_t}) i_t + \psi(s,\xi)\varsigma_u \quad (8)$$

Where ς_u

$$\varsigma = \frac{L(s,\boldsymbol{\beta})}{H(s,\boldsymbol{\beta})} = \frac{1 + l_1 s^{-1} + l_2 s^{-2} + \cdots + l_{n_l} s^{-n_l}}{1 + h_1 s^{-1} + h_2 s^{-2} + \cdots + h_{n_h} s^{-n_h}} \quad (9)$$

and $\xi \triangleq [l_1, \cdots, l_{n_l}, h_1, \cdots, h_{n_h}]$

The $\boldsymbol{\theta}$ denotes vector that accommodate parameterization, which consists of sub-vectors $\boldsymbol{\theta_1}, \cdots, \boldsymbol{\theta_n}$ to parameterize model blocks.

$$\boldsymbol{\theta} = [\boldsymbol{\theta_1}^T, \boldsymbol{\theta_2}^T, \cdots, \boldsymbol{\theta_n}^T, \xi^T]^T \quad (10)$$

Equations (8) and (10) shows concatenation of H-W model, which its LTI model order and the nonlinear system blocks are assumed to be known [37]. In what follows, H-W model from equations (8)-(10) could be coined if n=2, and $W_2(s,\delta_2) = 1$, which implies $n_{x_2} = n_{y_2} = 0, y_0^2 = 1$. The output of model is given by

$$o(t) = \frac{\sum_{t=1}^{n_L} L_t, \delta s^{-t}}{1 + \sum_{c=1}^{n_H} H_c, \delta s^{-c}} i_u \quad (11)$$

The challenge is how to optimize parameters $\boldsymbol{\theta}$ to forecast measured output $f_t(r_u, g_t)$ to be as transparent as observed output $\hat{f}_t(r_u, g_t)$ to forecast θ'. If fixed input and steady system is assumed, then r_u^t and o_u are also bounded, indicates that (8) is estimated to a transparent on polynomial according to (10). Specifically, if polynomial order is infinite, then (8) is exactly equals to (10), as demonstrated theoretically, but in practice high order of polynomial implies prone to disturbance and identification of model setting is probable [38]. This proposition poses a limitation to inverse method.

II. MATERIALS AND METHODS

A. Adaptive Neuro-fuzzy Inference System (ANFIS)

ANFIS is an artificial intelligence algorithm, which hybridizes Artificial Neural Network (ANN) and fuzzy logic networks to form Adaptive Neuro fuzzy inference System model [43], to address inherent drawbacks of individual networks. The major advantage of utilizing ANFIS algorithm, is the reliable modeling of complex non-linear characteristics [32], [43]. We constructed our ANFIS model using fuzzy Sugeno model from five layers, that are evaluated with weights of the week days as input *i*, whereas number of confirmed reported cases per day was used as the output *O*. The first order Sugeno fuzzy is activated, using randomly selected 80% and 20% of the dataset for both training and validation phases, respectively. ANFIS is extended to forecast number of confirmed cases of covid-19. The chosen parameters' values of ANFIS is described in Table I.

B. Hammerstein-Wiener Model Parameters Estimation

In this section, we described general error estimation procedure for deriving prediction of $\boldsymbol{\theta'_N}$ of parameter $\boldsymbol{\theta}$ described in H-W model in equations (8)-(10), according to our *N* number of input $\{i_u\}$ and output $\{o_u\}$ datasets. Thus, least squares cost function χ_N, can be set to

$$\boldsymbol{\theta'_N} = argmin\chi_N(\theta) \quad (12)$$

Where $\chi_N(\theta) = \sum_{u=1}^{N} \tau_t^2(\boldsymbol{\theta})$
and $\tau_t^2(\boldsymbol{\theta}) \triangleq o_u - o'_u|u-1|(\theta)$
$o'_u|u-1|(\theta)$ denotes best prediction of mean square [37] of o_u according to previous datasets and equation (10). However, disturbance $\{\varsigma_u\}$ remain independence.

$$o'_u|u-1|(\theta)(\boldsymbol{\theta}) = \psi^{(-1)}(s,\xi)(\prod_{u=1}^{n} Q_u\boldsymbol{\theta}) i_u + [1 - \psi^{-1}(s,\xi)] o_u \quad (13)$$

However, Eqs. (12)-(13) estimate θ'_N has non-convex and non-linearly parameterized optimization problem. Hence, this solution is not a closed form. Therefore, a general error estimation paired by gradient-based search according to Gauss-Newton which is attracted to local minima is proposed [37], [39]. This method ensures effective estimation approach. However, Gauss-Newton may have deviated to minimum, but we adopt procedures in [37] using L-M algorithm, due to it makes hasty move to low cost area and creeps to minimum. Therefore, this approach computes $\boldsymbol{\theta'_N}$ according to iterative gradient-based search.

1) Estimation Procedures: In this section, we extended Gauss-Newton algorithm. Let define vector $\varsigma(\theta)$ for error estimation residuals $\{\tau_u(\theta)\}$:

$$\boldsymbol{\zeta}(\boldsymbol{\theta}) \triangleq \begin{bmatrix} \tau_1\boldsymbol{\theta} \\ \vdots \\ \tau_N\boldsymbol{\theta} \end{bmatrix} \tag{14}$$

From this, local linear approximation is established

$$\boldsymbol{\zeta}(\boldsymbol{\theta}+\boldsymbol{d})(\approx)\boldsymbol{\zeta}(\boldsymbol{\theta}+\boldsymbol{J}(\boldsymbol{\theta})\boldsymbol{d} \tag{15}$$

With $\boldsymbol{d}$ as the minimizer to estimate cost function, and $\boldsymbol{J}(\boldsymbol{\theta}) \in \mathbb{R}^{N\times n}$ is the Jacobian of $\boldsymbol{\zeta}(\boldsymbol{\theta})$, with elements

$$(J)\boldsymbol{\theta} = \begin{bmatrix} \frac{\partial \boldsymbol{\zeta_1}(\boldsymbol{\theta})}{\partial\theta_1)} & \cdots & \frac{\partial \boldsymbol{\zeta_1}(\boldsymbol{\theta})}{\partial\theta_n)} \\ \vdots & & \vdots \\ \frac{\partial \boldsymbol{\zeta_N}(\boldsymbol{\theta})}{\partial\theta_1)} & \cdots & \frac{\partial \boldsymbol{\zeta_N}(\boldsymbol{\theta})}{\partial\theta_n)} \end{bmatrix} \tag{16}$$

Accordingly, $\boldsymbol{\theta}$ is local around

$$\begin{aligned}\chi_N(\boldsymbol{\theta}+\boldsymbol{d}) = \boldsymbol{\zeta^T}(\boldsymbol{\theta}+\boldsymbol{d})\boldsymbol{\zeta}(\boldsymbol{\theta}+\boldsymbol{d}) \approx \boldsymbol{\zeta^T}(\boldsymbol{\theta})\boldsymbol{\zeta}(\boldsymbol{\theta}) \\ + 2\boldsymbol{\zeta^T}(\boldsymbol{\theta})\boldsymbol{J}(\boldsymbol{\theta})\boldsymbol{d} + \boldsymbol{d}^T\boldsymbol{J}^T(\boldsymbol{\theta})\boldsymbol{d}\end{aligned} \tag{17}$$

However, cost function estimate fulfils

$$\boldsymbol{J}^T(\boldsymbol{\theta})\boldsymbol{J}(\boldsymbol{\theta})\boldsymbol{d} = -\boldsymbol{J}^T(\boldsymbol{\theta})\boldsymbol{\zeta}(\boldsymbol{\theta}) \tag{18}$$

Henceforth, inability of minimizer to reduce the cost function in local approximation, therefore, it is handle like search direction coupled for a point $\boldsymbol{\theta} + \mu\boldsymbol{d}$ assumes, such that

$$\chi_N(\boldsymbol{\theta} + \mu\boldsymbol{d}) < \chi_N(\boldsymbol{\theta}) \tag{19}$$

whereμ denotes $\mu \in \mathbb{R}$.
Therefore, the procedures brief check iterative search method for calculating parameter estimate using Gauss-Newton approach. Due to limitation, we extended L-M algorithm which is regularized version of the Gauss-Newton (Gn), with cost function approximation (21).

III. The Extended Levenberg-Marquardt (L-M) Algorithm

Levenberg-Marquardt algorithm is one kind of least square method which sum the advantages of gradient descent and the Gauss-Newton methods respectively to address their individual limitations. One special aspect of L-M algorithm is that, acts like Gauss-Newton when parameters are within their range of optimal values, whereas parameters outside optimal values acts like gradient descent [40]. Conventionally, choosing values only from estimated $\boldsymbol{\theta}$ is not a suitable option in a noisy observation, as many contributions of parameters in (22) are not considered by most techniques. Thus, we extend the L-M algorithm to minimize the entire function in (24), so that each parameter in the equation is considered important. According to nonlinearity nature of our data set and the H-W, this algorithm iteratively minimizes functions (12) and (13) according to the parameters θ. This iteration aim to realize a perturbation $\boldsymbol{d}$ according to parameters $\boldsymbol{\theta}$ which reduces sum of square errors χ_N. And also minimizes total sum of square errors across observed data and forecasted data. Jacobian J of this function relies on our chosen model not the dataset (16). Generally, cost function is given in (19).

$$\begin{aligned}\boldsymbol{J}_Reg(\boldsymbol{\theta}) &\approx \boldsymbol{\zeta}^T(\boldsymbol{\theta}+\boldsymbol{d})\boldsymbol{\zeta}(\boldsymbol{\theta})+\boldsymbol{d}) \\ &\approx \boldsymbol{\zeta}^T(\boldsymbol{\theta})\boldsymbol{\zeta}(\boldsymbol{\theta}) + 2\boldsymbol{\zeta}^T(\boldsymbol{\theta})\boldsymbol{J}(\boldsymbol{\theta})\boldsymbol{d} \\ &+ \boldsymbol{d}^T\boldsymbol{J}^T(\boldsymbol{\theta})\boldsymbol{d}\end{aligned} \tag{20}$$

$$\begin{aligned}\boldsymbol{J}_Reg(\boldsymbol{\theta}) &\approx \boldsymbol{\zeta}^T(\boldsymbol{\theta}+\boldsymbol{d})\boldsymbol{\zeta}(\boldsymbol{\theta}+\boldsymbol{d}) \\ &\approx \boldsymbol{\zeta}^T(\boldsymbol{\theta})\boldsymbol{\zeta}(\boldsymbol{\theta}) + 2\boldsymbol{\zeta}^T(\boldsymbol{\theta})\boldsymbol{J}(\boldsymbol{\theta})\boldsymbol{d} \\ &+ (\boldsymbol{d}^T\boldsymbol{J}^T(\boldsymbol{\theta})\boldsymbol{J}(\boldsymbol{\theta})\boldsymbol{d} + \lambda\mathbf{I})\end{aligned} \tag{21}$$

This function can now be minimized as the linear regularized problem.

$$\begin{aligned}\boldsymbol{\theta} =& \boldsymbol{\theta}^{'i} + \boldsymbol{\zeta}^T(\boldsymbol{\theta}^{'i})\boldsymbol{\zeta}(\boldsymbol{\theta}^{'i}) + 2\boldsymbol{\zeta}^T(\boldsymbol{\theta}^{'i})\boldsymbol{J}(\boldsymbol{\theta}^{'i})\boldsymbol{d} \\ &+ \lambda(\boldsymbol{d}^T\boldsymbol{J}^T\boldsymbol{\theta}^{'i})\boldsymbol{J}(\boldsymbol{\theta}^{'i})\boldsymbol{d}\end{aligned} \tag{22}$$

This equation can be employed as the next iterate, which gives the iteration

$$\boldsymbol{\theta}^{'(i+1)} = \boldsymbol{\theta}^{'i} + \Delta\boldsymbol{\theta}^{'(i+1)} \tag{23}$$

$$\begin{aligned}\Delta\boldsymbol{\theta}^{'(i+1)} =& (\boldsymbol{d}^T\boldsymbol{J}^T(\boldsymbol{\theta}^{'i})\boldsymbol{J}(\boldsymbol{\theta}^{'i})\boldsymbol{d} + \lambda\mathbf{I}) + \boldsymbol{\zeta}^T(\boldsymbol{\theta}^{'i})\boldsymbol{\zeta}(\boldsymbol{\theta}^{'i}) \\ &+ 2\boldsymbol{\zeta}^T(\boldsymbol{\theta}^{'i})\boldsymbol{J}(\boldsymbol{\theta}^{'i})\boldsymbol{d}\end{aligned} \tag{24}$$

We can now normalize the regularized function approximation using diagonal values of

$$(\boldsymbol{d}^T\boldsymbol{J}^T(\boldsymbol{\theta}^{'i})\boldsymbol{J}(\boldsymbol{\theta}^{'i})\boldsymbol{d})$$

However, the regularization term is replaced with $\lambda diag$, with Jacobian containing diagonal entries, then scaled L-M algorithm is formulated as

$$\begin{aligned}\Delta\boldsymbol{\theta}^{'(i+1)} =& (\boldsymbol{d}^T\boldsymbol{J}^T(\boldsymbol{\theta}^{'i})\boldsymbol{J}(\boldsymbol{\theta}^{'i})\boldsymbol{d}) + \lambda diag(\boldsymbol{d}^T\boldsymbol{J}^T(\boldsymbol{\theta}^{'i})\boldsymbol{J}(\boldsymbol{\theta}^{'i})\boldsymbol{d}) \\ &+ \boldsymbol{\zeta}^T(\boldsymbol{\theta}^{'i})\boldsymbol{\zeta}(\boldsymbol{\theta}^{'i}) \\ &+ 2\boldsymbol{\zeta}^T(\boldsymbol{\theta}^{'i})\boldsymbol{J}(\boldsymbol{\theta}^{'i})\boldsymbol{d}\end{aligned} \tag{25}$$

Moreover, step $\boldsymbol{d}$ is assessed during each iteration i, and difference between χ_N and $\chi_N(\boldsymbol{\theta} + \mu\boldsymbol{d})$ is noted. This step is accepted once metric E is greater than a user-specified threshold, $\xi_{10} > 0$ (26)-(27). This serve as true metric to measure improvement in χ_N due to L-M upgrade, expecting that approximations are precise [41].

$$E(\boldsymbol{d}) = \frac{\chi_N - \chi_N(\boldsymbol{\theta} + \mu\boldsymbol{d})}{(o-o')^T\mathbf{R}(o-o') - (o-o'-\boldsymbol{J}\boldsymbol{d})^T\boldsymbol{R}(o-o'-\boldsymbol{J}\boldsymbol{d})} \tag{26}$$

$$E(\boldsymbol{d}) = \frac{\chi_N - \chi_N(\boldsymbol{\theta} + \mu\boldsymbol{d})}{\boldsymbol{d}^T(\lambda_c diag\boldsymbol{J}^T\boldsymbol{R}(o-o')\mathbf{d} + (\boldsymbol{J})^T\mathbf{R}(o-o'(\boldsymbol{\theta}))} \tag{27}$$

If an iteration has $E(\boldsymbol{d}) > \xi_{10}$, then $\boldsymbol{\theta} + \boldsymbol{d}$ is adequately superior to $\boldsymbol{d}$, therefore $\boldsymbol{d}$ is substituted with $\boldsymbol{\theta}$ + $\boldsymbol{d}$, and λ is decreased by a factor. Else, λ is improved by a factor, and steps in Algorithm 1 continues to next iteration. Fig. 2 illustrates step response of the dataset. Major steps of adopted method are given in Algorithm 1. The parameters of adopted model are calculated with metrics described in section IV-C.

Algorithm 1 Levenberg-Maquardt-Scaled Algorithm

Input:
Initial parameter guesses $\theta_0 \in \mathbb{R}^n$
Data $\boldsymbol{N}$,
Function $\boldsymbol{f(\theta)}$,
Jacobian $\boldsymbol{J_\theta}$,
Initial damping λ^0,
Parameter θ,

$$\xi \in [0, 1]$$

Output:
Estimate $\boldsymbol{\theta'_N}$ // parameter estimate
Initialize $i \longleftarrow 0$ and $\lambda \longleftarrow \lambda^0$
For $i \longleftarrow 0$ $\lambda \longleftarrow \lambda^0$ **do**
Repeat
Calculate the candidate parameter update:
If scale gradient, **then**

$$\begin{aligned}\Delta\boldsymbol{\theta}^{'(i+1)} = &\left(\boldsymbol{d}^T\boldsymbol{J}^T\left(\boldsymbol{\theta}^{'(i)}\right)\boldsymbol{J}\left(\boldsymbol{\theta}^{'(i)}\right)\boldsymbol{d}\right)\\ &+\lambda\text{diag}\left(\boldsymbol{d}^T\boldsymbol{J}^T\left(\boldsymbol{\theta}^{'(i)}\right)\boldsymbol{J}\left(\boldsymbol{\theta}^{'(i)}\right)\boldsymbol{d}\right)\\ &+\boldsymbol{\zeta}^T\left(\boldsymbol{\theta}^{'(i)}\right)\boldsymbol{\zeta}\left(\boldsymbol{\theta}^{'(i)}\right)\\ &+2\boldsymbol{\zeta}^T\left(\boldsymbol{\theta}^{'(i)}\right)\boldsymbol{J}\left(\boldsymbol{\theta}^{'(i)}\right)\boldsymbol{d}\end{aligned}$$

else initialize conventional LM algorithm

$$\begin{aligned}\Delta\boldsymbol{\theta}^{'(i+1)} = &\left(\boldsymbol{d}^T\boldsymbol{J}^T\left(\boldsymbol{\theta}^{'(i)}\right)\boldsymbol{J}\left(\boldsymbol{\theta}^{'(i)}\right)\boldsymbol{d}+\lambda\mathbf{I}\right)\\ &+\boldsymbol{\zeta}^T\left(\boldsymbol{\theta}^{'(i)}\right)\boldsymbol{\zeta}\left(\boldsymbol{\theta}^{'(i)}\right)\\ &+2\boldsymbol{\zeta}^T\left(\boldsymbol{\theta}^{'(i)}\right)\boldsymbol{J}\left(\boldsymbol{\theta}^{'(i)}\right)\boldsymbol{d}\end{aligned}$$

end if
If the cost function

$$\chi_N\left(\boldsymbol{\theta}+\mu\boldsymbol{d}\right) < \chi_N\left(\boldsymbol{\theta}\right)$$

do simulate the candidate and decrement λ;$\boldsymbol{\theta'}^{(i+1)} = \boldsymbol{\theta}^{'(i)} + \Delta\boldsymbol{\theta'}^{(i+1)}$

$$\lambda \longleftarrow \lambda/\theta$$

Initialize $i \longleftarrow i+1$
else
discard the candidate and increment λ

$$\lambda \longleftarrow \theta\lambda$$

end if
until converged
max $\left|\frac{d}{E}\right| < \xi$ or max $\left|\boldsymbol{J}^T R(o-o'\right| < \xi$ or if *reduced* χ_N exist
Return $\boldsymbol{\theta'_N} = \boldsymbol{\theta}^{'(i)}$, R^2, *reduced* χ_N

IV. Datasets, Performance Metrics, Experiment and Results

A. Description of Datasets

The Corona Virus Disease (COVID -19) was reported first within continent of Africa in Egypt on 15/03/2020 [1]. This study utlized data set of Africa, which is a publicly available repository published by [42], contained reported confirmed cases of COVID-19 across West African region, as shown in figure 2. West Africa has a population of 281,202,440 based on 2018 estimate and has 16 countries which comprised of Benin republic, Burkina-faso, Cape verde, Gambia, Ghana, Guinea, Guinea Bissau, Ivory Coast, Liberia, Mali, Mauritania, Niger, Nigeria, Senegal, Sierra Leone, and Togo [44], respectively. As of 29th April 2020, total of 9413 cases of COVID-19 were recorded in West Africa, this region recorded first case on 15th March 2020, within this period, there is drastic rise in number of infected cases (virus spread). Virus spreads follow an Exponential growth model (EGM) at an earlier stage as depicted by characteristics plot in Figure 2. An intrinsic EGM can be estimated from a nonlinear system model using H-W initialized from Levenberg-Marquardt algorithm.

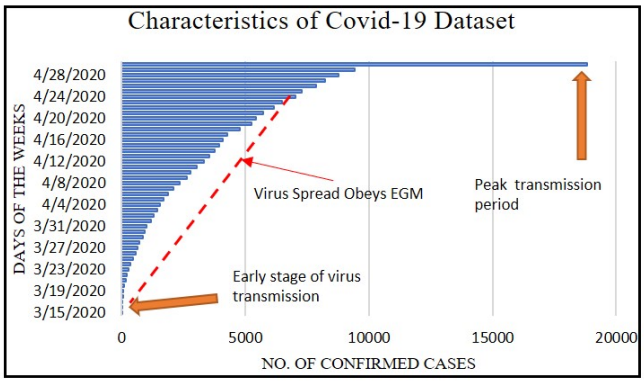

Fig. 2: Sample of Confirmed cases of COVID-19 Dataset

Furthermore, confirmed reported cases of COVID-19 in West African region [42] is normalized, and numerically calibrated. Then data set are randomly divided into 80% for calibration part and 20% for validation part, respectively. The carefully selected variables are number of confirmed reported cases as output O of three adopted models and time as input i to models, respectively. Offsets and linear trends are not removed from dataset before training, this is to ensure ability of the extended model to handle complex data. The three models H-W, ANFIS, and HW-LM algorithm are constructed in MATLAB R2020a software. The selected parameter values for these models are details in Table I.

B. Parameter Settings

The following parameters in Table I are chosen for three adopted models design.

C. Performance Metrics

In this section, we described evaluation metrics to evaluate models' performance. Variables $O_i, O'_i, S,, \theta, \sigma_r^2$ and O_a denotes observed data, forecasted data, number of samples, number of parameters, and average observed data, respectively.

1) Root Mean Square Error (RMSE):

$$\textbf{RMSE} = \sqrt{\frac{1}{S}\sum_{i=1}^{S}(O'_i - O_i)^2} \tag{28}$$

2) Mean Absolute Percentage Error (MAPE):

$$\textbf{MAPE} = \frac{1}{S}\sqrt{\sum_{i=1}^{S}\left|\frac{O'_i - O_i}{O'_i}\right|} \tag{29}$$

3) Mean Absolute Error (MAE):

$$\mathbf{MAE} = \frac{1}{S}\sqrt{\sum_{i=1}^{S}|O'_i - O_i|} \tag{30}$$

4) Root Mean Squared Relative Error (RMSRE):

$$\mathbf{RMSRE} = \frac{1}{S}\sqrt{\sum_{i=1}^{S}(\frac{O'_i - O_i}{O'_i})^2} \tag{31}$$

5) Mean Absolute Deviation (MAD) :

$$\mathbf{MAD} = \frac{\sum_{i=1}^{S}(O_i - O_{a_i})}{S} \tag{32}$$

6) Coefficient of Determination (R^2) :

$$\mathbf{R}^2 = 1 - \frac{\sum_{i=1}^{S}(O_i - O'_i)^2}{\sum_{i=1}^{S}(O_i - O_{a_i})^2} \tag{33}$$

Furthermore, we reported HW-LM model's simplicity, flexibility and degree of fitness according to following two metrics: Akaike's Information Criterion correction (AICc), and Nash-Sutcliffe model efficiency index (N-S).

7) Akaike's Information Criterion (AICc): AIC estimate degree of information lost for a model [46]. If small number of datasets are employed for model development, AIC index may likely to overfit, thus corrected AIC (AICc) is formulated to handle AIC overfit. AICc metrics evaluate quality of model according to flexibility of structure and amount of mean deviation [43]. It is obtained during model's verification of unseen observations [45], [43]. Therefore, low value of AICc describes best model. AICc is computed as follows:

$$\mathbf{AICc} = \frac{(2\theta S + (S ln(\sigma_r^2)(S - \theta - 1))}{S - \theta - 1} \tag{34}$$

8) Nash-Sutcliffe model efficiency index (η_{N-S}) : Nash-Sutcliffe model efficiency is defined to evaluate level of model fitness and deviation, with index value from $-\infty$ to 1 [43]:

$$\eta_{N-S} = 1 - [\frac{\sum_{i=1}^{S}(O_i - O'_i)^2}{\sum_{i=1}^{S}(O_i - O'_i)^2}] \times 100 \tag{35}$$

D. Results

In this section, we present performance results of the three adopted models according to calibrated and verified confirmed cases of COVID-19 virus across West African region. According to well-defined evaluation metrics of section IV-C, it is demonstrated that optimized H-W model tracks exponential growth pattern of COVID-19 virus spread in most of complex data pattern, therefore results of optimized H-W model outperforms conventional H-W and ANFIS models respectively. This indicates that HW-LM optimization algorithm is a promising tool to covid-19 dataset and with flexible and soft computing attributes.

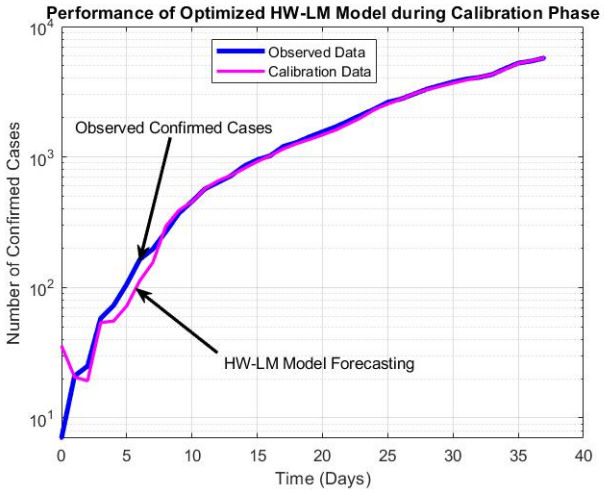

Fig. 3: Performance of optimized HW-LM Model on COVID-19 data during calibration phase

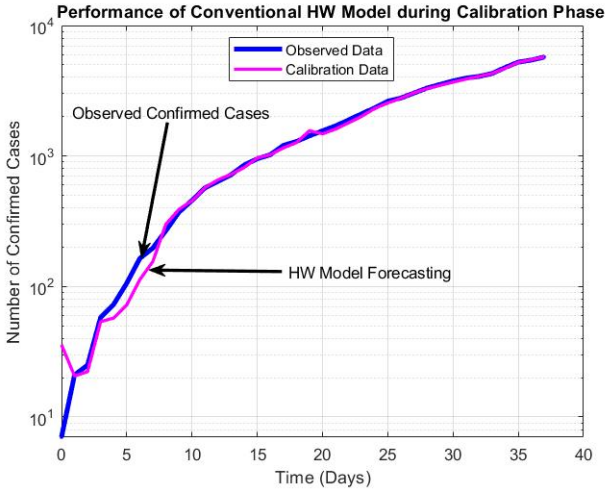

Fig. 4: Performance of conventional HW Model on COVID-19 data during calibration phase

1) Performance of models during calibration Phase: Table II, and Figs. 3 to 5 details the performance of the adopted models during calibration phase. It can be observed from Fig. 5, that early stage of virus transmission, ANFIS model performed poorly to track approximate data pattern due to ANFIS parameters' estimation complexity, small number of dataset, and nonlinearity among dataset. However when virus transmission obeys exponential growth model, ANFIS model demonstrates smooth performance better than two considered models. These confirmed that most machine and deep learning models suffers parameters estimation problem and require large amount of dataset to achieve promising results. Furthermore, conventional HW model adjust to complex data pattern at early stage of virus spread, though overfitted at some certain spikes, however when a gradient search algorithm is introduced in HW model, a smooth and fast convergence is achieve faster than other two adopted models (H-W and ANFIS). This can be observed in Table II.

2) Performance of models during Validation Phase: In this section, validation performance of the adopted models are presented in Table III, and Figs. 6 to 8. It is very

TABLE I: Initial Parameters used for the models

Layer	Parameter	Value
HW Model	*No of iterations*	300
HW-LM Model	*Tolerance*	$1.0 \times 10^{-}5$
	Regularization Weighting	1
	Input delay	1
	Piecewise linear break points	10
	No of poles and zeros	3 and 2
	Lambda	[0,1]
	Max epochs	300
	No of fuzzy rules	14
ANFIS Model	*Initial step*	0.01
	Gaussmf	-
	Error goal	0
	No of parameters	222
	Initial Step	0.001
	Step reduction	2
LM algorithm	*Initial gamma*	0.0001
	Regularization	10
	Max bisections	25
	Initial Gn Tolerance	$1.0 \times 10^{-}4$

TABLE II: Evaluation Results for the COVID-19 dataset during Calibration Phase

Method	**RMSE**	**MAPE**	**MAE**	**RMSRE**	R^2	**Time**
HW-LM	46.467	0.153	36.159	0.405	0.999	0.78
HW	54.53	1.896	49.313	0.561	0.898	0.79
ANFIS	60.170	3.622	38.733	16.514	0.991	-

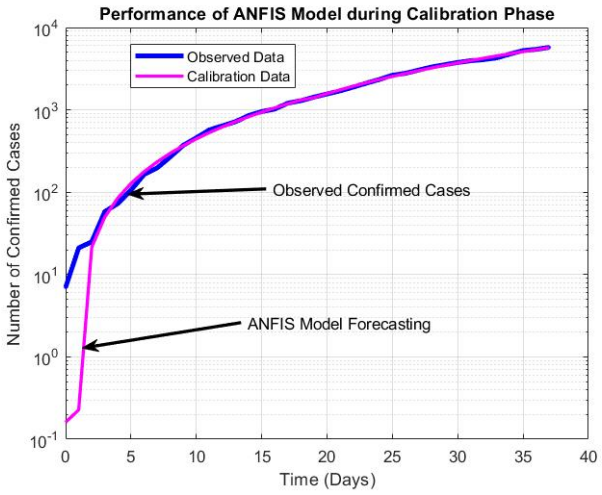

Fig. 5: Performance of ANFIS Model on COVID-19 data during calibration phase

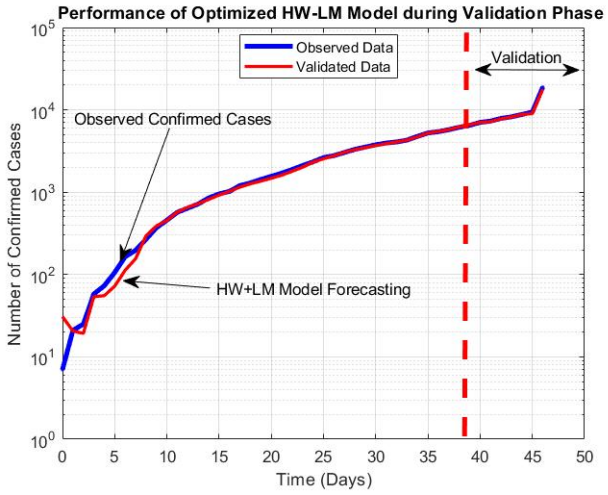

Fig. 6: Performance of optimized HW-LM Model on COVID-19 data during validation phase

clear to see from Fig. 8 that ANFIS model lack good generalization capability to complex pattern of COVID-19 dataset. However, conventional H-W model tracks unseen COVID-19 dataset with low overfitting as illustrated in Fig. 7, compared to ANFIS model. According to Fig. 6, optimized HW-LM achieve outstanding performance, due to gradient search makes hasty move to low cost area and creeps to minimum. HW with fast LM optimization algorithms will certainly make novel forecasting model to nonlinear dataset such as COVID-19 epidemic diseases. However, HW-LM model's generalization capability to complex data pattern is depicted in Fig. 6.

E. Comparison between the performance of optimized HW-LM model and state-of-the-art method

According to Table IV, our adopted model is compared based on work in [28]. The comparison is made base on number of dataset (NODS), inference time and statistical evaluation metrics adopted by this paper. The best result is bold-faced.

Moreover, HW-LM model has superior performance when compared to other two models, therefore it is chosen for further analysis according to two metrics: Corrected Akaike's information criterion (AICc) index and Nash-Sutcliffe model efficiency index. AICc is adopted due to our small sample size (S) and number of different parameters (θ). However, value of AICc is obtained from Equation 34, with 1.86.

TABLE III: Evaluation Results for the COVID-19 dataset during Validation Phase

Method	RMSE	MAPE	MAE	RMSRE	R^2	Time
HW-LM	165.085	0.127	68.046	0.364	0.998	0.78
HW	198.31	0.999	97.493	0.912	0.861	0.79
ANFIS	905.771	2.249	191.534	8.892	0.631	-

TABLE IV: Comparison of the adopted model with the state-of-the-art model

Method	NODS	RMSE	MAPE	MAE	RMSRE	R^2	Time
HW-LM model Ours	**18826**	**165.08**	**0.127**	**68.046**	**0.364**	**0.998**	**0.78**
FPASSA [28]	72528	5779	4.79	4271	0.07	0.9645	23.3

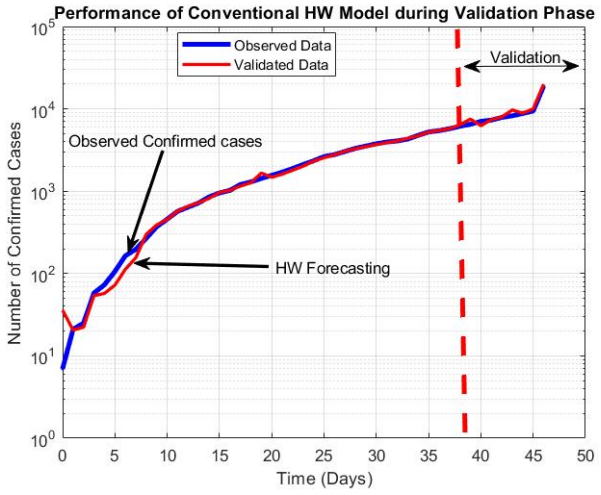

Fig. 7: Performance of conventional HW Model on COVID-19 data during validation phase

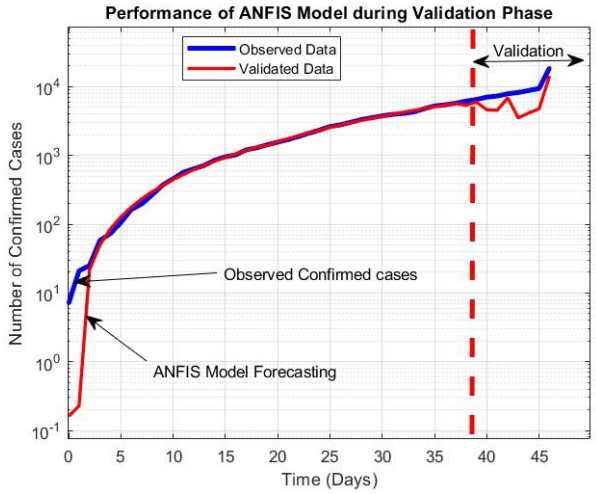

Fig. 8: Performance of ANFIS Model on COVID-19 data during validation phase

We observed that AICc from HW-LM model achieved best result, which lead to model flexibility. Loss function of HW-LM model is obtained as 2.85×10^{-7}, this shows smaller criterion, and smaller criterion depict model accuracy. In addition, final prediction error of HW-LM Model is obtained as 2.815×10^{-6}, this value demonstrates that HW-LM model has good generalization quality to COVID-19 data. However, HW-LM model fitness is achieved as 98.81%. The value of η_{N-S} is obtained through Equation 35, with 98.99% model accuracy. Therefore, the obtained results demonstrates that HW-LM algorithm is a promising tool to nonlinear dataset such as COVID-19 and conform with current-state-of-the-art method.

V. Conclusions

In this work, we initialized gradient search optimization algorithm as potential enabler in conventional Hammerstein-Wiener model to handle complex parameters estimation. This extended model is realized according to proper parameters chosen. However, the adopted model is validated on confirmed reported cases of COVID-19 virus across 16 West African countries. The optimized model is a good forecasting tool for COVID-19 dataset. In terms of HW model parameters, LM optimization algorithm handles model parameters very well, which overcomes noise inherited from conventional HW model.

The superiority of HW-LM model is apparently depicted in Figs. (3) and (6), during calibration and validation phases. It shows that by comparison, there is significant reduce in virus spread from first phase to second phase in the west African region and that may be due to prevention measures taken by countries such as partial lockdown, ban of public gathering, ban of in and out migration, total lockdown to provide social distance, and awareness by health personnel. In addition, our adopted model exhibits low computational cost, flexibility with good accuracy to small dataset. Our model would serve as prediction tool of epidemic diseases and could be extended to different fields.

Acknowledgment

Auwal Bala Abubakar would like to thank the Department of Mathematics and Applied Mathematics, Sefako Makgatho Health Sciences University, Ga-Rankuwa, Pretoria, Medunsa-0204, South Africa. The fourth author would like to thank Phetchabun Rajabhat University.

References

[1] T. A. Ghebreyesus, "WHO Director-General's opening remarks at the media briefing on COVID-19 - 11 March 2020," BBC Media, accessed Jul. 25, 2020.

[2] Gralinski, E. Lisa, and D. V. Menachery, "Return of the Coronavirus: 2019-nCoV," Viruses MDPI, vol. 12, no. 2, pp128-135, 2020.

[3] Ahmed, A. Qanta, Memish and A. Ziad, "The cancellation of mass gatherings (MGs)? Decision making in the time of COVID-19," Travel Medicine and Infectious Disease, Elsevier, vol. 2020, Article ID 101631, 2020.

[4] Chan, J. Fuk-Woo, Y. Shuofeng, Kok, Kin-Hang, To, K. Kai-Wang, Chu, Hin, Yang, Jin, Xing, Fanfan, Liu, Jieling, Yip, C. Chik-Yan, Poon, R. Wing-Shan, "A familial cluster of pneumonia associated with the 2019 novel coronavirus indicating person-to-person transmission: a study of a family cluster," The Lancet, vol. 395, no. 10223, pp514-523, 2020.

[5] K. Roosa, Y. Lee, R. Luo, A. Kirpich, R. Rothenberg, J. M. Hyman, P. Yan and G. Chowell, "Real-time forecasts of the COVID-19 epidemic in China from February 5th to February 24th, 2020," Infectious Disease Modelling, vol. 5, no. 2020, pp256-263, 2020.

[6] Z. Liu, P. Magal, O. Seydi, and G. Webb, "Predicting the cumulative number of cases for the COVID-19 epidemic in China from early data," ArXiv preprint Article ID 2002.12298, 2020.

[7] S. Zhao, P. Cao, D. Gao, Z. Zhuang, M. K. Chong, Y. Cai, J. Ran, K. Wang, L. Yang, D. He, and M. H. Wang, "Epidemic growth and reproduction number for the novel coronavirus disease (COVID-19) outbreak on the Diamond Princess cruise ship from January 20 to February 19, 2020: A preliminary data-driven analysis," SSRN Electronic Journal, vol.2020, Article ID 3543150, pp256-263, 2020.

[8] K. Mizumoto, K. Kagaya, A. Zarebski, and G. Chowell, "Estimating the asymptomatic proportion of coronavirus disease 2019 (COVID-19) cases on board the Diamond Princess cruise ship, Yokohama, Japan, 2020," Eurosurveillance:European Centre for Disease Prevention and Control, vol. 25, no. 10, pp1-5, 2020.

[9] T. A. Ghebreyesus, "One World: Together At Home;WHO Director-General's opening remarks at the media briefing on COVID-19," WHO, Geneva, Switzerland, 2020.

[10] R. N. Thompson, T. D. Hollingsworth, V. Isham, D. Arribas-Bel, B. Ashby, T. Britton, P. Challenor, L. H. Chappell, H. Clapham, N. J. Cunniffe, and A. P. Dawid Dai, "Key questions for modelling COVID-19 exit strategies," Proceedings of the Royal Society B, vol. 287, no. 1932, pp19-34, 2020.

[11] Z. Hermanowic and W. Slav, "Forecasting the Wuhan coronavirus (2019-nCoV) epidemics using a simple (simplistic) model," MedRxiv, Cold Spring Harbor Laboratory Press, 2020.

[12] S. Zhao, S. S. Musa, Q. Lin, J. Ran, G. Yang, W. Wang, Y. Luo, L. Yang, D. Gao, D. He, M. H. Wang, "Estimating the unreported number of novel coronavirus (2019-nCoV) cases in China in the first half of January 2020: a data-driven modelling analysis of the early outbreak," IMA Journal of Clinical Medicine, vol. 9, no. 2, p388, 2020.

[13] S. Zhao, Q. Lin, J. Ran, S. S. Musa, G. Yang, W. Wang, Y. Luo, D. Gao, L. Yang, D. He, M. H. Wang, "Preliminary estimation of the basic reproduction number of novel coronavirus (2019-nCoV) in China, from 2019 to 2020: A data-driven analysis in the early phase of the outbreak," International Journal of Advanced Science and Technology, vol. 92, no. 2020, pp214-217, 2020.

[14] T. Liu, J. Hu, J. Xiao, G. He, M. Kang, Z. Rong, L. Lin, H. Zhong, Q. Huang, A. Deng, and W. Zeng, "Time-varying transmission dynamics of Novel Coronavirus Pneumonia in China," BioRxiv;Cold Spring Harbor Laboratory, 2020.

[15] S. M. Jung, A. R. Akhmetzhanov, K. Hayashi, N. M. Liinton, Y. Yang, B. Yuang, T. Kobayashi, R. Kinoshita, and H. Nishiura, "Real-time estimation of the risk of death from novel coronavirus (COVID-19) infection: inference using exported cases," Journal of clinical medicine, vol. 9, no.2, p523, 2020.

[16] J. T. Wu, K. Leung, and G. M. Leung, "Nowcasting and forecasting the potential domestic and international spread of the 2019-nCoV outbreak originating in Wuhan, China: a modelling study,"The LAncet, vol. 395, no.10225, pp689-697, 2020.

[17] Q. Zhao, Y. Chen, and D. S. Small, "Analysis of the epidemic growth of the early 2019-nCoV outbreak using internationally confirmed cases," MedRxiv, 2020.

[18] C. Anastassopoulou, L. Russo, A. Tsakris, and C. Siettos, "Data-based analysis, modelling and forecasting of the COVID-19 outbreak," PloS one, vol. 15, no. 3, pe0230405, 2020.

[19] J. Sun, X. Chen, Z. Zhang, S. Lai, B. Zhao, H. Liu, S. Wang, W. Huan, R. Zhao, M. T. Ng, and Y. Zheng, "Forecasting the long-term trend of COVID-19 epidemic using a dynamic model," Scientific Reports, vol. 10, no.1, pp1-10, 2020.

[20] F. Yanuar and A. Zetra, "Length-of-Stay of Hospitalized COVID-19 Patients Using Bootstrap Regression," IAENG International Journal of Applied Mathematics, vol. 51, no.3, pp799-810, 2021.

[21] P. Hendikawati, Subanar, Abdurakhman and Tarno, "ANFIS Performance Evaluation for Predicting Time Series with Calendar Effects," IAENG International Journal of Applied Mathematics, vol. 51, no.3, pp587-598, 2021.

[22] L. Sun, X. Zhao, and J. Liu, "The Extinction and Persistence of a Stochastic SIQR Epidemic Model with Vaccination Effect," IAENG International Journal of Applied Mathematics, vol. 51, no.3, pp777-784, 2021.

[23] S. K. Bandyopadhyay, and S. Dutta, "Machine learning approach for confirmation of covid-19 cases: Positive, negative, death and release," MedRxiv, 2021.

[24] N. Yudistira, "COVID-19 growth prediction using multivariate long short term memory," ArXiv preprint, Article ID 2005.04809, 2020.

[25] K. ElDahshan, E. K. Elsayed, and H. Mancy, "Enhancement Semantic Prediction Big Data Method for COVID-19: Onto-NoSQL," IAENG International Journal of Computer Science, vol. 47, no.4, pp613-622, 2020.

[26] K. Suebyat, P. Oyjinda, S. A. Konglok, and N. Pochai, "A Mathematical Model for the Risk Analysis of Airborne Infectious Disease in an Outpatient Room with Personal Classification Factor," Engineering Letters, vol. 28, no.4, pp1331-1337, 2020.

[27] Y. Kang, and X. Abdurrahman, "Dynamic Behavior of a Brucellosis Infection Model with the Effect of Infected Dogs," IAENG International Journal of Applied Mathematics, vol. 50, no.3, pp636-642, 2020.

[28] M. A. Al-Qaness, A. A. Ewees, H. Fan, and M. AbdElAziz, "Optimization method for forecasting confirmed cases of COVID-19 in China," Journal of Clinical Medicine, vol. 9, no.3, p674, 2020.

[29] A. Ahmad, S. Garhwal, S. K. Ray, G. Kumar, S. J. Malebary, and O. M. Barukab, "The number of confirmed cases of covid-19 by using machine learning: Methods and challenges," Archives of Computational Methods in Engineering;Springer, vol. 28, no. 4, pp1-9, 2020.

[30] L. Sersour, T. Djamah, and M. Bettayeb, "Nonlinear system identification of fractional Wiener models," Nonlinear Dynamics, vol. 92, no. 4, pp1493-1505, 2018.

[31] M. R. Rahmani, and M. Farrokhi, " Nonlinear dynamic system identification using neuro-fractional-order Hammerstein model," Transactions of the Institute of Measurement and Control, vol. 40, no. 13, pp3872-3883, 2018.

[32] S. B. Abdullahi, and M. S. Gaya, "Forecasting of HOSR for Different Mobile Carriers in Kano Using Conventional and Intelligent Techniques," International Journal of New Computer Architectures and Their Applications, vol. 9, no. 1, pp1-11, 2019.

[33] A. A. Gonzalez, R. Bertschinger, and D. Saupe, "Modeling VO_2 and VCO_2 with Hammerstein-Wiener Models," 4th International Congress on Sport Sciences Research and Technology Support, pp134-140, 2016.

[34] E. Shokrollahi, A. A. Goldenberg, J. M. Drake, K. W. Eastwood and M. Kang, "Application of a Nonlinear Hammerstein-Wiener Estimator in the Development and Control of a Magnetorheological Fluid Haptic Device for Robotic Bone Biopsy," Actuators, vol. 7, no. 4, p83, 2018.

[35] J. Zambrano, J. Sanchis, J. M. Herrero, and M. Martinez, "WH-EA: an evolutionary algorithm for Wiener-Hammerstein system identification," Complexity, vol. 2018, 2018.

[36] K. K. Xu, H. D. Yang, and C. J. Zhu, "A novel extreme learning machine-based Hammerstein-Wiener model for complex nonlinear industrial processes," Neurocomputing, vol. 358, no. 2019, pp246-254, 2019.

[37] A. Wills, and B. Ninness, "Generalised Hammerstein–Wiener system estimation and a benchmark application," Control Engineering Practice, vol. 20, no. 11, pp1097-1108, 2012.

[38] E. W. Bai, "A blind approach to the Hammerstein–Wiener model identification," Automatica, vol. 38, no. 6, pp967-979, 2002.

[39] F. Rosenqvist and A. Karlstrom, "Realisation and estimation of piecewise-linear output-error models," Automatica, vol. 41, pp545-551, 2005.

[40] H. P. Gavin, "The Levenberg-Marquardt algorithm for nonlinear least squares curve-fitting problems," Department of Civil and Environmental Engineering, Duke University, pp1-19, 2019.

[41] M. K. Transtrum, B. B. Machta, and J. P. Sethna, "Why are nonlinear fits to data so challenging?," Physical Review Letters, vol. 104, no. 6, Article ID 060201, 2010.

[42] D. Worldometer, "COVID-19 coronavirus pandemic," World Health Organization, www. worldometers, 2020.

[43] S. B. Abdullahi, K. Muangchoo, A. B. Abubakar, A. H. Ibrahim, A. O. Kazeem, "Data-Driven AI-Based Parameters Tuning Using Grid Partition Algorithm for Predicting Climatic Effect on Epidemic Diseases," IEEE Access, vol. 9, no.2021, pp55388–55412, 2021.

[44] C. Poletto, M. F. Gomes, A. P. yPiontti, L. Rossi, L. Bioglio, D. L. Chao, I. M. Longini, M. E. Halloran, V. Colizza, A. Vespignani, "Assessing the impact of travel restrictions on international spread of the 2014 West African Ebola epidemic," Eurosurveillance, vol. 19, no.42, pp20936, 2014.

[45] K. P. Burnham, D. R. Anderson, and K. P. Huyvaert, "AIC model selection and multimodel inference in behavioral ecology: some background, observations, and comparisons," Behavioral Ecology and Sociobiology, vol. 65, no. 1, pp23-35, 2011.

[46] A. Hirotugu, "A new look at the statistical model identification, " IEEE Transactions on Automatic Control, vol. 19, no. 6, pp716-723, 1974.

Sunusi Bala Abdullahi received the B.Sc. and M.Sc. degrees in electronics from the Bayero University Kano (BUK), Nigeria. He is currently pursuing the Ph.D. degree with the King Mongkut's University of Technology Thonburi, Thailand. His current research focuses on computer vision, artificial intelligence, nonlinear optimization and their applications in human motion analysis, data analysis, and social signal processing.

Abdulkarim Hassan Ibrahim was born in Sokoto, Nigeria. He received the B.Sc. degree in mathematics from Usmanu Danfodiyo University Sokoto, Nigeria, and the Ph.D. degree in applied mathematics from the King Mongkut's University of Technology Thonburi, Bangkok, Thailand. He has authored and coauthored several research articles indexed in either Scopus or web of science. His current research interests include numerical optimization and image processing. In August 2018, he was awarded the Petchra Pra Jom Klao Scholarship to study the Ph.D. degree.

Auwal Bala Abubakar received the master's degree in mathematics and the Ph.D. degree in applied mathematics from the King Mongkut's University of Technology Thonburi, Thailand, in 2015. He is currently a Lecturer with the Department of Mathematical Sciences, Faculty of Physical Sciences, Bayero University Kano, Nigeria. He is the author of more than 40 research articles. His main research interest includes methods for solving nonlinear monotone equations with application in signal recovery and image restoration.

Abhiwat Kambheera is currently a Lecturer with the Department of Mathematics and Computing Sciences, Faculty of Science and Technology, Phetchabun Rajabhat University, Phetchabun, Thailand. He obtained his Master degree in mathematics education in Burapha University in 2015. He has published research papers in various international journals and attended international conferences. His research interest includes Mathematical computation in sciences and their applications.